INTERNATIONAL JOURNAL FOR NUMERICAL METHODS IN FLUIDS, VOL. 21, 973–979 (1995)

VISUALIZATION OF FLOWS BY FEM USING SIX-NODE TRIANGULAR ELEMENT: FREE SURFACES AND FLOW PATTERNS OF AN EXTRUSION PROCESS

YOJI SHIMAZAKI

Department of Civil Engineering, Tokai University, 1117 Kitakaname Hiratsuka, Kanagawa, 259–12 Japan

SUMMARY

A simple extrusion process for Newtonian and power-law fluids is analysed. Marker particles are introduced to analyse the fluid flow motions. Area co-ordinates of six-node triangular element are used to determine the marker position in the element. With this element, the solution algorithm becomes simple compared with the one using the linear triangular element. The differences in flow and swell patterns between the two fluids are described.

KEY WORDS: finite element method; transient flow; power-law fluid; extrudate swell; marker particles

1. INTRODUCTION

A finite element method using a six-node triangular isoparametric element is studied to analyse transient power-law fluid flow motion, in which marker particles are introduced to represent the motion. For determining the marker positions in an element, area co-ordinates of the triangular element are used. Shiojima *et al.*[1,2] have introduced the area co-ordinates of a linear triangular element, which are utilized for finding the new marker position, into a four-node quadrilateral isoparametric element. The two kinds of interpolation systems, however, give a complicated solution algorithm and may lead to unexpected errors in the calculated results. Also, this method requires a finer mesh arrangement to obtain an accurate results. This implies that a large amount of extra storage may be required for the analysis. With the six-node element the determination of the new marker position in an element becomes simple compared with using the linear triangular element. This is because we use three mid-node points on each side of the triangle to make them correspond to three area co-ordinates. In other words, if only one sign of the area co-ordinates for the marker is minus, it moves towards the direction of one of the mid-node points. Since only two elements share the mid-node, we can easily determine the new element for the marker. Also, the velocities at the six nodes obtained by the calculation can be directly used for the interpolation of the marker velocity.[3] The markers are arranged when the mesh is generated.

In this paper we describe a simple extrusion processes for Newtonian and power-law fluids. Marker particles are used to show the extruded free surfaces. The flow patterns are visualized by arranging markers inside the transient flow.

2. GOVERNING EQUATIONS

The equations of time-dependent creeping flow of incompressible Newtonian and power-law fluids without body forces in rectangular Cartesian co-ordinates are as follows:

CCC 0271–2091/95/100973–07

Received 2 June 199
Revised 29 October 199

equilibrium

$$\rho u_{i,t} + \sigma_{ij,\,j} = 0 \tag{1}$$

continuity (incompressible fluids)

$$u_{i,i} = \varepsilon_{ii} = 0. \tag{2}$$

constitutive relationships

$$\varepsilon_{ij} = (u_{i,j} + u_{j,i})/2, \tag{3}$$

$$\sigma_{ij} = -p\delta_{ij} + \sigma'_{ij}, \tag{4}$$

$$\sigma'_{ij} = 2\mu\varepsilon_{ij}, \tag{5}$$

with

$$\mu = \text{constant} \quad \text{(Newtonian fluids)},$$

$$\mu = \eta_0[1 + (\lambda\dot{\gamma})^a]^{(n-1)/a} \quad \text{(power-law fluids)},$$

$$\dot{\gamma} = \sqrt{(\varepsilon_{ij}\varepsilon_{ij})},$$

boundary conditions

$$u_i = \bar{u}_i, \tag{6}$$

$$v_j\sigma_{ij} = \bar{T}_i, \tag{7}$$

where ρ is the density, μ is the viscosity coefficient, u_i is the velocity component in the x_i-direction, p is the pressure, σ_{ij} is the total stress, σ'_{ij} is the deviatoric stress, η_0 is the zero-share-rate viscosity, λ is a time constant, n is the power-law exponent, a is a dimensionless parameter and v_j is the component of the unit outward normal vector on the boundary.

3. FINITE ELEMENT METHOD

3.1. Velocity calculation

We interpolate the velocity and pressure as

$$\tilde{u}_i = N_k\hat{u}_{ki}, \qquad \tilde{p} = M_m\hat{p}^m, \tag{8a,b}$$

where $\hat{u}_{ki}$, $\hat{p}^m$ are the velocity and pressure at nodal points respectively. N_k and M_m are shape functions. Galerkin's method applied to equation (1), with the boundary conditions of equation (7), gives

$$\rho\int_v Nu_{i,t}\,\mathrm{d}v + \int_v N_{,j}\,\sigma_{ij}\,\mathrm{d}v = \int_s v_j\sigma_{ij,}\,\mathrm{d}s. \tag{9}$$

We now approximate equation (2) using the small number κ (10^{-12}). The penalty function method[4] gives

$$\frac{1}{\kappa}\int_v Mu_{i,i}\,\mathrm{d}v + \int_v Mp\,\mathrm{d}v = 0. \tag{10}$$

Substituting p in equation (10) into equation (9) and using equation (8) gives, in matrix form,

$$[C]\{\hat{u}_{,t}\} + [K]\{\hat{u}\} = \{F\}, \tag{11}$$

where $[C]$ and $[K]$ are from the first and second terms and $\{F\}$ is from the right-hand side of equation (9). For two-dimensional problems

$$[C] = \begin{bmatrix} C_{xx} & \\ & C_{yy} \end{bmatrix}, \qquad [K] = \begin{bmatrix} K_{xx} & K_{xy} \\ K_{yx} & K_{yy} \end{bmatrix}, \tag{12}$$

where

$$[C_{xx}] = \left[\int_v N\rho N \, \mathrm{d}v\right], \tag{13}$$

$$[C_{yy}] = \left[\int_v N\rho N \, \mathrm{d}v\right], \tag{14}$$

$$\begin{aligned}[K_{xx}] = &\left[\int_v \left(\frac{\partial N}{\partial x} 2\mu \frac{\partial N}{\partial x} + \frac{\partial N}{\partial y} \mu \frac{\partial N}{\partial y} \boxed{+ \frac{N}{x} 2\mu \frac{N}{x}}\right) \mathrm{d}v\right] \\ &- \frac{1}{\kappa}\left[\int_v \left(\frac{\partial N}{\partial x} M \boxed{+ \frac{N}{x} M}\right) \mathrm{d}v\right] \left[\int_v MM \, \mathrm{d}v\right]^{-1} \times \left[\int_v \left(M \frac{\partial N}{\partial x} \boxed{+ M \frac{N}{x}}\right) \mathrm{d}v\right],\end{aligned} \tag{15}$$

$$\begin{aligned}[K_{xy}] = &\left[\int_v \left(\frac{\partial N}{\partial y} \mu \frac{\partial N}{\partial x}\right) \mathrm{d}v\right] - \frac{1}{\kappa}\left[\int_v \left(\frac{\partial N}{\partial x} M \boxed{+ \frac{N}{x} M}\right) \mathrm{d}v\right] \left[\int_v MM \, \mathrm{d}v\right]^{-1} \\ &\times \left[\int_v \left(M \frac{\partial N}{\partial y}\right) \mathrm{d}v\right] \\ = &[K_{yx}],\end{aligned} \tag{16}$$

$$[K_{yy}] = \left[\int_v \left(\frac{\partial N}{\partial y} 2\mu \frac{\partial N}{\partial y} + \frac{\partial N}{\partial x} \mu \frac{\partial N}{\partial x}\right) \mathrm{d}v\right] - \frac{1}{\kappa}\left[\int_v \frac{\partial N}{\partial y} M \mathrm{d}v\right] \left[\int_v MM \mathrm{d}v\right]^{-1} \left[\int_v \left(M \frac{\partial N}{\partial y}\right) \mathrm{d}v\right]. \tag{17}$$

The 'boxed' terms in equations (15) and (16) must be added when axisymmetric problems are considered. In this case the x-co-ordinate corresponds to the radial direction and the y-co-ordinate is the axis perpendicular to the radius. The θ-method[5] for the time derivative in equation (11) gives

$$\left[\frac{1}{\Delta t}[C] + \theta[K]\right]\{u\}_{t+\Delta t} = \{F\}_{\text{avg}} + \left[\frac{1}{\Delta t}[C] + (1-\theta)[K]\right]\{u\}_t, \tag{18}$$

$$\{F\}_{\text{avg}} = \{(1-\theta)\{F\}_t + \theta\{F\}_{t+\Delta t}\}. \tag{19}$$

3.2. *Marker method*

Figure 1 shows the area co-ordinates for the six-node triangular element. The position P can be determined by the three co-ordinates ξ, η and ξ.[5]

We now introduce marker particles in the finite elements to represent the fluid flow motion. Figure 2

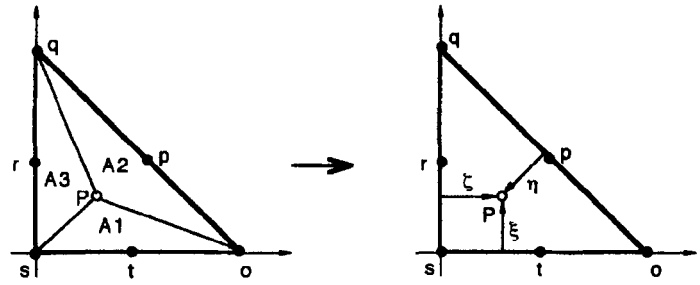

Figure 1. Area co-ordinates

shows the position of a marker at time t in the six-node triangular isoparameteric element. The marker position at time $t + \Delta t$ becomes

$$(x_i)_{t+\Delta t} = (x_i)_t + \int_t^{t+\Delta t} (\tilde{u}_i)_t \, dt, \tag{20}$$

$$(\tilde{u}_i)_t = [N_k]\{\hat{u}_{ki}\}_t, \tag{21}$$

where $(x_i)_t$ is the marker position and $(\tilde{u}_i)_t$ the marker velocity at time t and $\hat{u}_{ki}$ is the velocity at the nodal point. With the shape functions N_k expressed in area co-ordinates (ξ, η, ζ) and the nodal point position $\hat{x}_{ki}$ in global co-ordinates, the marker position $(x_i)_{t+\Delta t}$ becomes

$$(x_i)_{t+\Delta t} = [N_k]\{\hat{x}_{ki}\}, \tag{22}$$

where the shape functions N_k for the six-node triangular element are

$$N_1 = (2\xi - 1)(\xi), \qquad N_2 = 4(\xi)(\eta), \qquad N_3 = (2\eta - 1)(\eta), \tag{23a–c}$$

$$N_4 = -4(\zeta)(\eta), \qquad N_5 = (\zeta)(2\eta + 2\xi - 1), \qquad N_6 = -4(\xi)(\zeta). \tag{23d–f}$$

Because $(x_i)_{t+\Delta t}$ is known for equation (20) and $\hat{x}_{ki}$ represents the co-ordinate values of the six nodal points in an element, we can calculate the marker position in triangular co-ordinates (ξ, η, ζ) by the Newton–Raphson method. According to the signs of the calculated ξ, η, and ζ, the new element of the marker is determined. If $\xi < 0$, $\eta \geqslant 0$ and $\zeta \geqslant 0$, for example, the marker N in Figure 2 moves into element L.

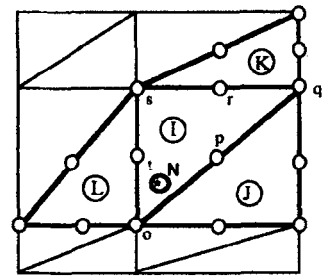

Figure 2. Marker N and elements I, J, K and L

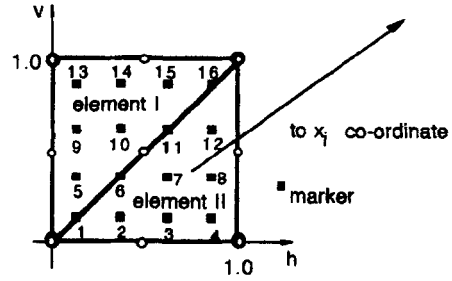

Figure 3. Markers in elements I and II

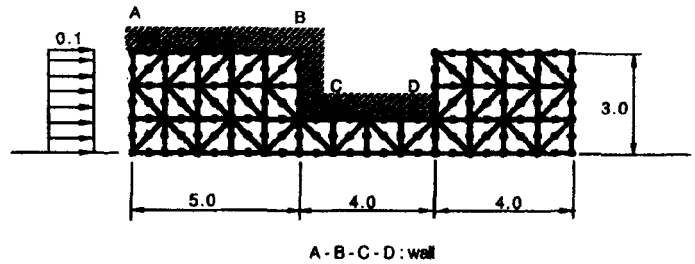

Figure 4. Axisymmetric problem

3.3. Automatic marker generation

The markers are arranged automatically. For each marker we have to know its co-ordinates x_i and the element to which it belongs. These can be obtained when the finite element mesh is generated. Figure 3 shows a unit-square element to be mapped into x_i-co-ordinates. The element is divided into two triangles. In the figure 16 markers are arranged in two elements.

4. EXTRUSION PROBLEM

Figure 4 shows an axisymmetric extrusion problem. The problem consists of 62 elements and 161 nodal points.

The initially arranged markers are shown in Figure 5. The number of markers arranged in the region is 304.

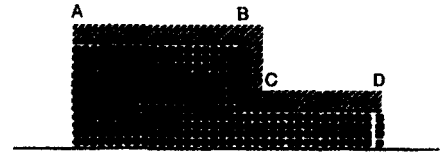

Figure 5. Initial marker positions ($t = 0$)

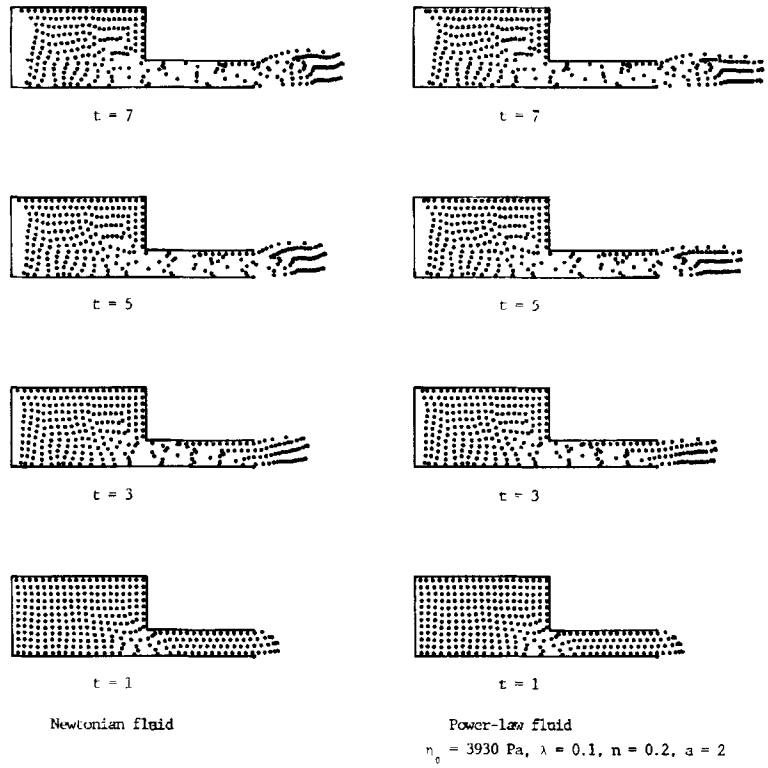

Figure 6. Calculated results

The material properties used for the Newtonian fluid are $\rho = 1{\cdot}0$ and $\mu = 1{\cdot}0$. We choose $\theta = 0{\cdot}75$ and $\Delta t = 0{\cdot}5$. To obtain better accuracy and to avoid numerical instability, Δt is divided into n intervals (from 20 to 50) for finding the new marker position. To proceed with the transient analysis, we assume that the free surface—which is physically a line consisting of the forefront markers and also a place to specify the boundary conditions—is located on the boundary line between an element with forefront markers and one without them. Because the traction force along the side is zero, we do not need to specify any boundary values and this assumption does not affect the visualization of the free surface as a marker front. It should be noted that for problems of practical importance we need to have a finer mesh arrangement than that in Figure 4.

Figure 6 illustrates the results obtained by this method. The difference between Newtonian and power-law fluid flows at each time step is shown.

5. CONCLUSIONS

Marker particles were used to represent the fluid flow motion of transient incompressible creeping flows. The six-node triangular (second-order) element was used to move the marker from element to element. With this element a simple solution algorithm for the marker was obtained.

The extrusion processes of Newtonian and power-law fluid flows were calculated. The free surfaces and flow patterns of the two fluid flows were described.

APPENDIX: CALCULATION OF EQUATION (22)

We rewrite equation (22) with respect to the area co-ordinates (ξ, η, ζ) and the global co-ordinates (x, y). Using equation (23), it becomes

$$2(x_1 + x_5 - 2x_6)\xi^2 + 4(x_2 - x_4 + x_5 - x_6)\xi\eta + 2(x_3 - 2x_4 + x_5)\eta^2$$
$$+(-x_1 - 3x_5 + 4x_6)\xi + (-x_3 + 4x_4 - 3x_5)\eta + x_5 = X, \tag{24}$$

$$2(y_1 + y_5 - 2y_6)\xi^2 + 4(y_2 - y_4 + y_5 - y_6)\xi\eta + 2(y_3 - 2y_4 + y_5)\eta^2$$
$$+(-y_1 - 3y_5 + 4y_6)\xi + (-y_3 + 4y_4 - 3y_5)\eta + y_5 = Y, \tag{25}$$

$$\xi + \eta + \zeta = 1, \tag{26}$$

where x_{1-6} and y_{1-6} are the global co-ordinate values at the six nodal points in an element. The equation for (ξ, η, ξ) by the Newton–Raphson method is

$$\begin{bmatrix} a_{11} & a_{12} \\ a_{21} & a_{22} \end{bmatrix} \begin{Bmatrix} \Delta\xi \\ \Delta\eta \end{Bmatrix} = \begin{Bmatrix} X \\ Y \end{Bmatrix} - \begin{Bmatrix} f_x \\ f_y \end{Bmatrix}, \tag{27}$$

$$\xi_{i+1} = \xi_i + \Delta\xi, \qquad \eta_{i+1} = \eta_i + \Delta\eta, \qquad \zeta_{i+1} = 1 - \xi_{i+1} - \eta_{i+1}, \tag{28a–c}$$

where

$$a_{11} = 4(x_1 + x_5 - 2x_6)\xi + 4(x_2 - x_4 + x_5 - x_6)\eta + (-x_1 - 3x_5 + 4x_6),$$

$$a_{12} = 4(x_2 - x_4 + x_5 - x_6)\xi + 4(x_3 - 2x_4 + x_5)\eta + (-x_3 + 4x_4 - 3x_5),$$

$$a_{21} = 4(y_1 + y_5 - 2y_6)\xi + 4(y_2 - y_4 + y_5 - y_6)\eta + (-y_1 - 3y_5 + 4y_6),$$

$$a_{22} = 4(y_2 - y_4 + y_5 - y_6)\xi + 4(y_3 - 2y_4 + y_5)\eta + (-y_3 + 4y_4 - 3y_5)$$

and f_x and f_y corresponds to the left-hand sides of equations (24) and (25) respectively.

REFERENCES

1. T. Shiojima, Y. Shimazaki and Daiguji, 'Finite element analysis of creeping flows using marker particles', *Int. j. numer. methods fluids*, **11**, 397–404 (1990).
2. T. Shiojima, Y. Shimazaki and Daiguji, 'Analyses of transient viscous fluid creeping flows with free surfaces', *Proc. JSME*, **86-1356A**, 2365–2369 (1987).
3. Y. Shimazaki and S. Hovanotayan 'A free surface analysis for transient creeping flow problems', *Proc. JSCE, Struct. Eng./ Earthq. Eng.*, **11**, 79–82 (1994).
4. F. Kikuchi and M. P. Navarro, 'An iteration method for the mixed formulation of parameter dependent problem related to the Stokes equations'. *Comput. Mech.*, 141–151 (1986).
5. O. C. Zienkiewicz, *The Finite Element Method*, 3rd edn, McGraw-Hill, New York, 1977.